Downloaded from www.annualreviews.org. University of Chicago Libraries (ar-129425) IP: 128.135.43.97 On: Tue, 03 Dec 2024 18:25:25

Annual Review of Condensed Matter Physics

Machine Learning for Climate Physics and Simulations

Ching-Yao Lai,[1] Pedram Hassanzadeh,[2] Aditi Sheshadri,[3] Maike Sonnewald,[4] Raffaele Ferrari,[5] and Venkatramani Balaji[6]

[1]Department of Geophysics, Stanford University, Stanford, California, USA; email: cyaolai@stanford.edu

[2]Department of Geophysical Sciences and Committee on Computational and Applied Mathematics, University of Chicago, Chicago, Illinois, USA

[3]Department of Earth System Science, Stanford University, Stanford, California, USA

[4]Department of Computer Science, University of California, Davis, California, USA

[5]Department of Earth, Atmospheric, and Planetary Sciences, Massachusetts Institute of Technology, Cambridge, Massachusetts, USA

[6]Schmidt Sciences, New York, NY, USA

Annu. Rev. Condens. Matter Phys. 2025. 16:343–65

The *Annual Review of Condensed Matter Physics* is online at conmatphys.annualreviews.org

https://doi.org/10.1146/annurev-conmatphys-043024-114758

Copyright © 2025 by the author(s). All rights reserved

Keywords

climate, physics-informed machine learning, machine learning-informed physics, equation discovery, parameterization, emulator

Abstract

We discuss the emerging advances and opportunities at the intersection of machine learning (ML) and climate physics, highlighting the use of ML techniques, including supervised, unsupervised, and equation discovery, to accelerate climate knowledge discoveries and simulations. We delineate two distinct yet complementary aspects: (*a*) ML for climate physics and (*b*) ML for climate simulations. Although physics-free ML-based models, such as ML-based weather forecasting, have demonstrated success when data are abundant and stationary, the physics knowledge and interpretability of ML models become crucial in the small-data/nonstationary regime to ensure generalizability. Given the absence of observations, the long-term future climate falls into the small-data regime. Therefore, ML for climate physics holds a critical role in addressing the challenges of ML for climate simulations. We emphasize the need for collaboration among climate physics, ML theory, and numerical analysis to achieve reliable ML-based models for climate applications.

Review in Advance. Changes may still occur before final publication.

Downloaded from www.annualreviews.org. University of Chicago Libraries (ar-129425) IP: 128.135.43.97 On: Tue, 03 Dec 2024 18:25:25

1. INTRODUCTION

Model: a representation of a system to make predictions; can be physics-based, ML-based, or coupled

Neural network (NN): function approximators parameterized by function operations and parameters γ, that are optimized to minimize specified cost functions $\mathcal{L}$

Simulation: physics-based models solved numerically

Emulator: a subset of models that fit the data, bypassing solving physics-based equations

Machine learning (ML) has led to breakthroughs in various areas, from playing Go to text generated with large language models (LLM) and, more recently, to weather forecasting (1–5). Different from Go and LLM, the language scientists use to understand and simulate weather and climate has been equations rooted in fundamental physics. Physics-based equations, often differential equations, are essential to simulate systems where direct observations are limited and noisy—even more so for projections of future climates where data are altogether unavailable (**Figure 1**). Recently, ML has emerged as an alternative tool for predictive modeling as well as improving the understanding of climate physics (**Figure 2**). For instance, physics-free ML models such as neural networks (NNs), which are universal approximators of functions (12) and operators (13), trained on data from observations or physics-based simulations have demonstrated a remarkable ability to perform accurate nowcasting (14) with lead time of a few hours, weather prediction (15) with lead times of several days, and El Niño forecast with lead times of a year (16). It remains an open question if some of the strategies and success in these short-time predictions can be applied to improve climate projections, i.e., to estimate changes in the statistics of weather events (e.g., return periods of heat waves or tropical cyclones) in the next decades, centuries, and beyond.

1.1. Weather Versus Climate: Nonstationarity

The success story of ML for prediction (Section 3.2) has been primarily showcased in weather forecasting (17). Followed by initial attempts started in 2019 (e.g., 18–24), by 2022–2023 ML weather models (often called emulators; Section 3.2) achieve, at a fraction of the computational cost, similar or better forecast skills than state-of-the-art physics-based weather prediction models (e.g., 1–5, 25). This success has generated excitement about using ML to improve climate projections as well. Yet, climate projections involve major additional challenges (26, 27). In weather forecasting, we have a constant stream of real-time and historical data for training ML-based emulators (*lower right* of **Figure 1*a***) to make predictions for a few weeks, where the statistics can be assumed to be stationary. In climate, we are often interested in predicting the climate's forced

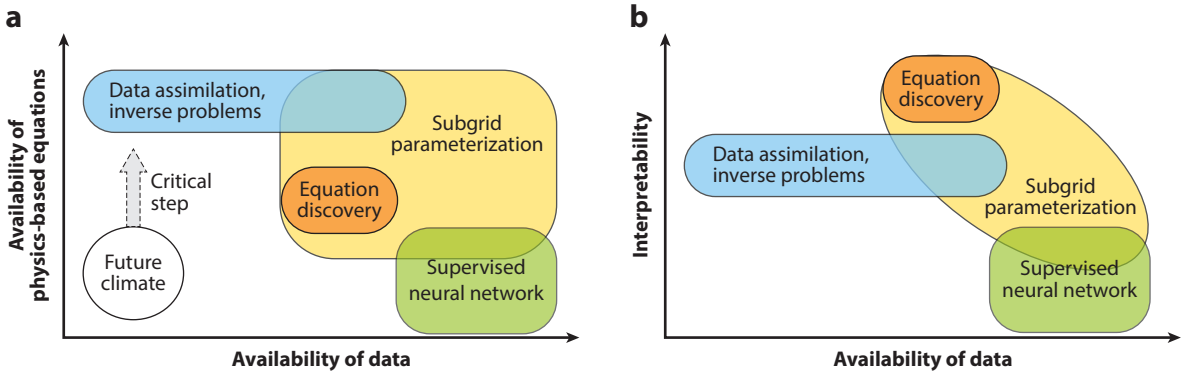

Figure 1

Conceptual diagram of ML applications in climate sciences with respect to the availability of existing physics-based equations, availability of data, and interpretability. We explain different components of this figure throughout this article. (*a*) Existing physics-based equations and data are two sources of information used for training ML models. (*b*) More physics-based equations are not necessarily more interpretable, e.g., existing numerical weather predictions. However, equation discovery usually comes with regularization techniques to find the simplest set of equations capturing the dominant behavior of the system, enhancing interpretability. Abbreviation: ML, machine learning.

Review in Advance. Changes may still occur before final publication.

Downloaded from www.annualreviews.org. University of Chicago Libraries (ar-129425) IP: 128.135.43.97 On: Tue, 03 Dec 2024 18:25:25

Machine learning for climate physics

Data-informed knowledge discovery

a Dimensionality reduction

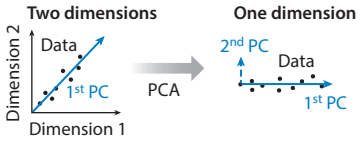

b Supervised versus unsupervised

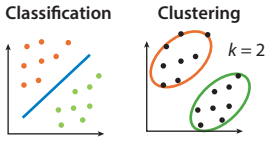

c Discover ocean dynamical regimes with clustering and validation

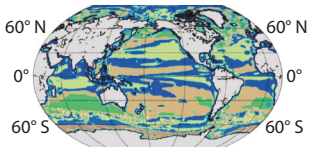

Data-informed model discovery

Example: $\dot{\boldsymbol{z}} \equiv [\dot{x}, \dot{y}, \dot{z}]^T = \boldsymbol{f}(\boldsymbol{z}(t), \boldsymbol{\theta})$, where $\boldsymbol{z}(t)$ are the states, t is time, $\boldsymbol{\theta}$ are model parameters

	Parametric estimation, $\boldsymbol{\theta}$	State estimation, $\boldsymbol{z}(t)$	Structural estimation, $\boldsymbol{f}$
Goal	Discover **parameters** $\boldsymbol{\theta}$ of a mathematical model that best fit a given dataset.	Discover **states** $\boldsymbol{z}(t)$ of a system given sparse, noisy, and discrete data.	Discover a **mathematical model** $\boldsymbol{f}$ that best fits a given dataset.
Example	EKI	Physics-informed neural networks, physics-informed neural operator	Sparse regression (e.g., SINDy), genetic algorithm
Given	$x(t)$, $y(t)$, $z(t)$ at lots of times, and mathematical form of the model $\boldsymbol{f}$	$x(t)$, $y(t)$ at sparse times, and the mathematical form of $\boldsymbol{f}$, including $\boldsymbol{\theta}$	$x(t)$, $y(t)$, $z(t)$ at lots of times
Predict	$\boldsymbol{\theta}$	State variables $x(t)$, $y(t)$, $z(t)$ at lots of times	The mathematical form of the model $\boldsymbol{f}$, including $\boldsymbol{\theta}$

d Parameter estimation

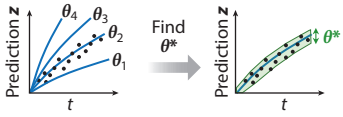

— Simulations from $\boldsymbol{f}(\boldsymbol{\theta})$
• Data

$\boldsymbol{\theta}^*$ Calibrated parameter with UQ

e UQ

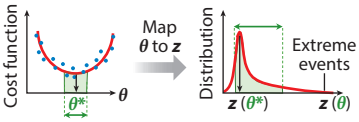

• Simulations from $\boldsymbol{f}(\boldsymbol{\theta})$ (expensive)
— Emulator (cheap)
↔ Plausible range of $\boldsymbol{\theta}$

$\boldsymbol{z}$ Prediction (e.g., sea-level rise in 100 years)

f State estimation example

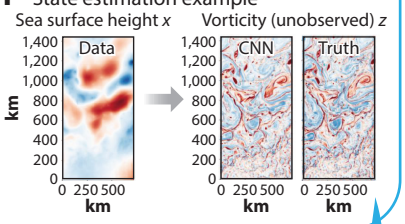

Machine learning for climate simulations

	SGS modeling	Machine-learning emulator
Goal	Learn an SGS model $\boldsymbol{\Pi}(\bar{\boldsymbol{z}})$ such that $\dot{\bar{\boldsymbol{z}}} = \boldsymbol{f}(\bar{\boldsymbol{z}}, \boldsymbol{\theta}) + \underbrace{\overline{\boldsymbol{f}(\boldsymbol{z})} - \boldsymbol{f}(\bar{\boldsymbol{z}})}_{\boldsymbol{\Pi}(\bar{\boldsymbol{z}})}$	Discover a model **parameterized by ML** that best fits a given dataset
Example	In LES $\bar{\boldsymbol{z}}$ is the coarse-grained $\boldsymbol{z}$, and $\boldsymbol{\Pi}$ includes Reynolds stress	ClimateBench, FourcastNet, Pengu Weather, GraphCast, ACE
Given	$\bar{\boldsymbol{f}}, \bar{\boldsymbol{\theta}}, \bar{\boldsymbol{z}}$ at lots of t and its high-resolution counterpart $\boldsymbol{z}$	Data of states from previous time step(s) $\boldsymbol{z}(t_i)$
Predict	$\boldsymbol{NN}(\bar{\boldsymbol{z}}, \gamma) = \boldsymbol{\Pi}(\bar{\boldsymbol{z}})$ or symbolic equation	State at future time step(s) $\boldsymbol{z}(t_{i+1})$

g Physics-informed ML

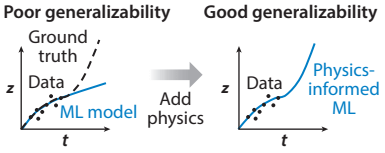

h Better generalization capacity via incorporating symmetries into NN

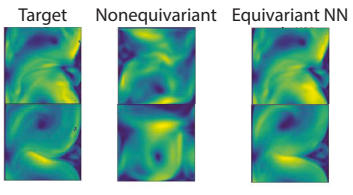

i Weather forecast via ML emulator

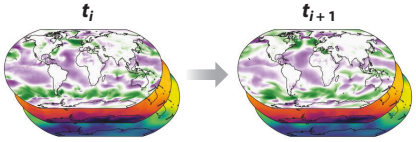

j SGS parameterization

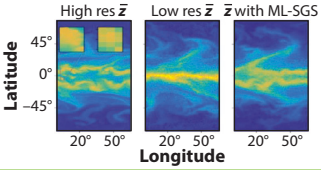

(*Caption appears on following page*)

Review in Advance. Changes may still occur before final publication.

Downloaded from www.annualreviews.org. University of Chicago Libraries (ar-129425) IP: 128.135.43.97 On: Tue, 03 Dec 2024 18:25:25

Figure 2 (*Figure appears on preceding page*)

An overview of the areas in which ML has played a role in uncovering climate physics and advancing climate simulations. Panels *c*, *f*, *h*, and *j* adapted with permission from Reference 6 (CC BY 4.0), Reference 7 (CC BY 4.0), Reference 8 (CC BY 4.0), and Reference 9 (CC BY 4.0), respectively. Panel *i* adapted from Reference 4; copyright 2023 AAAS. Abbreviations: ACE, AI2 Climate Emulator (10, 11); CNN, convolutional neural network; EKI, ensemble Kalman inversion; LES, large eddy simulation; ML, machine learning; NN, neural network; PC, principal component; PCA, principal component analysis; SGS, subgrid-scale; SINDy, sparse identification of nonlinear dynamics; UQ, uncertainty quantification.

response to changes in greenhouse gases in the atmosphere, leading to nonstationarity (28), e.g., climate with different mean and variability. ML models are not suited to predict the behavior of a system substantially different from the one they have been trained on. Yet we simply do not have observational data for the future (i.e., *lower left corner* in **Figure 1*a***) to train and validate future predictions; this is an issue for both ML and physics-based models but one expects the fundamental laws of physics to hold in the future as well. We summarize the nonstationary challenge and potential solutions, such as incorporating physics constraints, in Section 4.2. Furthermore, the long-term prediction of future climate involves the interactions between the atmosphere, ocean, cryosphere, land, and biosphere, which make the problem more challenging than short-term weather forecast.

1.2. Challenges in Understanding and Simulating Climate

The climate system consists of interacting processes that span orders of magnitude in spatial (from microns to planetary) and temporal (from seconds to centuries) scales. Simulating the climate system to resolve all these scales is computationally challenging. Due to its multiscale nature, representing physics in the underresolved scales (e.g., cloud microphysics, turbulence) in low-resolution climate simulations—referred to as subgrid-scale (SGS) parameterization—has been a central goal for climate scientists. ML has emerged as a promising alternative to SGS parameterization due to its ability to perform equation discovery and its desirable properties as universal function approximators, which do not require prior assumptions about the functional forms of the parameterization. We summarize recent advances of ML in SGS parameterization in Section 3.1 as well as its major challenges, such as interpretability in Section 4.1 (*lower right corner* of **Figure 1*b***) and uncertainty quantification (UQ) in Section 4.3. Without understanding what the ML model actually learns and the reasoning behind it, we cannot deduce when the ML model will generalize well to future climates. One approach to improve interpretability is discovering the closed-form equations that capture the data (Section 2.2.4.3; *upper side* of **Figure 1*b***). Equations have long been the language for physicists to develop understandings of the systems they govern. With the emergence of ML, ways to comprehend and extract knowledge from ML-based models are new areas of research. Several methods developed to understand what the ML model itself learns are detailed in Section 4.3.

We organize this article by focusing on two distinct goals through which ML is reshaping climate science: (*a*) ML for climate physics and (*b*) ML for climate simulations. The former focuses on utilizing the increasing availability of data from the Earth system to extract understandings, including knowledge discovery (Section 2.1) and data-driven model discovery (Section 2.2). The latter discusses recent advances in accelerating simulations, including data-driven parameterization (Section 3.1) and climate emulators (Section 3.2). Section 3.3 discusses methods used to add physical constraints to ML models. For inverse problems with sparse data (*upper left* of **Figure 1*a***) in the small-data regime including physical constraints is necessary to generalize prediction where data do not exist. Finally, the future climate also falls in the small-data regime, as no future observations exist. Along with an incomplete understanding of the physics of future

ML-based emulators: emulators that fit the data with ML models (e.g., deep neural networks), bypassing solving physics-based equations

Nonstationarity: systems with time-evolving statistical properties, so that a limited time series is not representative of the past or the future

Subgrid-scale (SGS) parameterization: a model to parameterize the relationship between the resolved states as a function of the unresolved (subgrid) state

Review in Advance. Changes may still occur before final publication.

Downloaded from www.annualreviews.org. University of Chicago Libraries (ar-129425) IP: 128.135.43.97 On: Tue, 03 Dec 2024 18:25:25

climate, it lies at the bottom left of **Figure 1*a***, making it the most challenging among others in **Figure 1*a***. Thus, predicting climate is not merely about accelerating simulation but essentially requires generating more physical knowledge than currently available, moving toward the tractable upper left regime of **Figure 1*a***. While training ML models to make accurate predictions faster than physics-based simulations, making previously challenging tasks computationally tractable, is an achievement, the ability to simulate does not equate to improved physical understanding (29). We stress that accurate and fast simulations or predictions are not sufficient; deeper physical understanding of the climate is necessary to address the climate modeling challenges.

Supervised learning: algorithms that learn a mapping from input data (features) to output labels based on the training examples provided

Unsupervised learning: algorithms that discover patterns, structures, or relationships within the input data (features) without explicit guidance from labeled examples

2. MACHINE LEARNING FOR CLIMATE PHYSICS

The increase in availability of data, from both observations and high-fidelity simulations, is a key driver for new physical insights. Below, we introduce two emerging trends of research using ML to improve our understanding of the climate physics using data: (*a*) Data-informed knowledge discovery, e.g., identifying patterns and dynamical regimes in high-dimensional, complex observations and simulations and (*b*) discovering data-informed predictive models.

2.1. Data-Informed Knowledge Discovery

Knowledge discovery (e.g., **Figure 2*a–c***), such as identifying coherent patterns of dynamical significance in spatiotemporal data, has long been a fundamental process for making discoveries in climate science. A classical example in atmospheric science is the identification of what we now call the El Niño Southern Oscillation (ENSO) by Walker in 1928 (30). Stationed in India during the British occupation, Walker employed an army of Indian clerks to conduct principal component analysis (PCA) by hand on all available data, decomposing it into orthogonal modes that revealed coherent structures associated with ENSO. Today, we have access to vast amounts of data, both observational and computational. Advanced ML techniques emerge as powerful pattern recognition tools that computationally scale well with increasing volumes of data. Off-the-shelf tools widely adopted in climate sciences include supervised learning methods [e.g., random forest, Gaussian process regression (GPR), and NN] and unsupervised learning methods such as autoencoders and clustering algorithms (e.g., k-means, self-organizing maps). Several of the above tools have been used in climate science for decades, long before deep learning took off.

2.1.1. Dimensionality reduction. Climate data often involve high-dimensional, nonlinearly correlated, spatial and temporal variables, such as temperature, pressure, and precipitation, across large geographical regions and long time periods. Dimensionality reduction has long been used for transforming high-dimensional climate data into a lower-dimensional space, which might be more amenable to physical interpretation and to develop reduced-order predictive models. PCA, also known as empirical orthogonal function (EOF), is one of the commonly used linear techniques for dimensionality reduction (**Figure 2*a***). Reducing decades of observational data into a few modes of variability, such as ENSO, has facilitated understanding of the underlying dynamics and even the robust detection and interpretation of the anthropogenic climate-change footprint (31, 32). However, traditional techniques such as PCA/EOF have major limitations, such as the lack of a dynamical meaning of the discovered modes and the linearity (33) (see also **Supplemental Text, Section II**).

ML techniques have the potential to address the linearity limitation. For example, autoencoders, a type of NN with high-dimensional input and output layers and a lower-dimension latent space, are powerful tools for dimensionality reduction. A single-layer autoencoder using linear activation functions is equivalent to PCA. In contrast, deep autoencoders with nonlinear activation functions have more expressive power in capturing the low-dimensional representation of the

Review in Advance. Changes may still occur before final publication.

Downloaded from www.annualreviews.org. University of Chicago Libraries (ar-129425) IP: 128.135.43.97 On: Tue, 03 Dec 2024 18:25:25

high-dimensional input (34, 35), and their applications to climate science have started to emerge. Shamekh et al. (36), interpreting the latent space of an autoencoder, developed of a new metric for cloud and precipitation organization, enabling the development of a parameterization for moist convection.

Markov models that describe the transition probability from one state to another are being applied to study the evolution of the climate system in a reduced space, possibly based on a PCA/EOF projection (37, 38). Latent variable models have also shown promise in numerical model analysis and predictive skill. For example, Wang et al. (39) improved ENSO prediction skill by using kernel analog forecasting [related to the Koopman operators (40), a mathematical technique to transform a nonlinear dynamical system into a linear one in a higher-dimensional space.].

2.1.2. Finding patterns in climate data. The task of finding patterns in climate data extends far beyond dimensionality reduction and is a fruitful area that still has much to be explored. For example, unsupervised methods like clustering (**Figure 2*b***) have been used to identify the balance between terms of the equations governing simulation data and to discover global ocean dynamical regions as parsimonious representations of the governing equations (6) (**Figure 2*c***).

Data from actual observations can often inspire new knowledge about climate systems (41). Supervised methods facilitate the utilization of vast amounts of satellite observations, such as reconstructing a pan-Arctic dataset of sea ice thickness during periods when data are unavailable (42), revealing the strong nonlinear interactions with ocean eddies (43), reconstructing ocean surface kinematics with sea-surface height measurements (7), and detecting icebergs to understand their contribution to the freshwater budget (44). Extracting information from remote-sensing data can fill missing gaps required to inform physics-based models. For example, the identification of ice fractures (underresolved in simulations) is needed to constrain parameters for modeling ice dynamics (45, 46). Some of the above tasks have long been done manually and often subjectively by scientists. ML offers an efficient alternative that can be easily scaled up to all available data that may be intractable otherwise and can be made easily accessible, reproducible, and transparent via open-source software. That said, the design of the loss functions is still subjective.

2.2. Data-Informed Model Discovery

Apart from distilling knowledge from data, physicists have been developing predictive models to describe observations for centuries. The utility of a model, if it accurately represents the observations, lies in its ability to make predictions when the data are unavailable, such as projections about the future. The crux of climate physics is creating trustworthy future predictions, and determining how to construct a model that faithfully describes the data are essential. It's worth noting that in traditional physical sciences, a model often takes the form of mathematical equations. In modern ML literature, a model can refer to functional operations (e.g., NNs) that parameterize relationships between specified input and output variables. For clarity, in this section, use of the term model discovery means the discovery of mathematical equations.

Here, we broadly classify three different ML approaches that have been used for finding models to describe climate data: parametric, state, and structural estimations (**Figure 2**). We use a dynamical-system example of the following form to illustrate the differences:

$$\frac{\mathrm{d}}{\mathrm{d}t}\boldsymbol{z}(t) = \boldsymbol{f}(\boldsymbol{z}(t), \boldsymbol{\theta}), \qquad 1.$$

where $\boldsymbol{z}(t) \in \mathbb{R}^n$ represents the states vector of the system that evolves with time $t \in \mathbb{R}$, and its evolution is dictated by the mathematical expression of the dynamics $\boldsymbol{f}$ and the model parameters $\boldsymbol{\theta}$ (see the sidebar titled The Lorenz 63 System for an example).

Review in Advance. Changes may still occur before final publication.

Downloaded from www.annualreviews.org. University of Chicago Libraries (ar-129425) IP: 128.135.43.97 On: Tue, 03 Dec 2024 18:25:25

THE LORENZ 63 SYSTEM

The Lorenz 63 system (47), a simplified mathematical model for atmospheric convection, is described by the following set of ordinary differential equations:

$$\frac{\mathrm{d}}{\mathrm{d}t}x = \mathrm{a}(y - x), \quad \frac{\mathrm{d}}{\mathrm{d}t}y = x(\mathrm{b} - z) - y, \quad \frac{\mathrm{d}}{\mathrm{d}t}z = xy - \mathrm{c}z,$$

where the model parameters $\boldsymbol{\theta} = [\mathrm{a}, \mathrm{b}, \mathrm{c}]$ are constants, and $\boldsymbol{z}(t) = [x(t), y(t), z(t)]$ are the time-evolving states.

2.2.1. Parametric estimation $\boldsymbol{\theta}$. Given a discrete dataset of states measured at discrete times t_i, i.e., $\{x(t_i), y(t_i), z(t_i)\}_{i=1}^N$, parametric estimation refers to predicting the free parameters $\boldsymbol{\theta} = [a, b, c]$ when the functional form of the mathematical model $\boldsymbol{f}(\boldsymbol{z}(t), \boldsymbol{\theta})$ is known. See **Figure 2*d***.

2.2.2. State estimation $\boldsymbol{z}$. State estimation involves predicting the state variables $\boldsymbol{z}(t)$ given the mathematical model $\boldsymbol{f}(\boldsymbol{z}(t), \boldsymbol{\theta})$, model parameters $\boldsymbol{\theta}$, and data $\{x(t_i), y(t_i), z(t_i)\}_{i=1}^N$. Estimating states is particularly useful for data interpolation when the available data are sparse in time or space, for data denoising, or for inversion when the predicted state is not measurable (e.g., **Figure 2*f***) and, thus, completely unavailable in the data library, e.g., predicting $\boldsymbol{z}(t)$ with data of $\{x(t_i), y(t_i)\}_{i=1}^N$.

2.2.3. Structural estimation $\boldsymbol{f}$. This is also referred to as equation discovery, reconstructing the complete mathematical expression of $\boldsymbol{f}(\boldsymbol{z}(t), \boldsymbol{\theta})$, including the free parameters $\boldsymbol{\theta} = [a, b, c]$ given only the discrete data $\{x(t_i), y(t_i), z(t_i)\}_{i=1}^N$. The determination of the model $\boldsymbol{f}(\boldsymbol{z}(t), \boldsymbol{\theta})$ fully relies on the data; therefore, dense data are often needed to guarantee the success of the algorithms.

Beyond these three categories, an emerging data-driven approach involves replacing $\boldsymbol{f}$ with an ML-based emulator. In this approach, instead of using equations, the dynamics $\boldsymbol{f}$ are represented by black-box ML models, as detailed in Section 3.2.

2.2.4. Algorithms and examples. In this section, we list a few examples that demonstrate how ML has influenced data-driven model discovery within the three categories described above; ensemble Kalman inversion (EKI) for parameter $\boldsymbol{\theta}$ estimation, physics-informed machine learning (PIML) for state $\boldsymbol{z}$ estimation, and equation discovery for structural $\boldsymbol{f}(\boldsymbol{z}, \boldsymbol{\theta})$ estimation.

2.2.4.1. Ensemble Kalman inversion. Here, we focus on one family of methods, EKI, as an example, as it is increasingly used in climate science. EKI (48) is a well-developed parameter estimation technique in the climate modeling community and has been used in various contexts such as convection, turbulence, and clouds (49–51), gravity waves (52), and ocean convection (53). EKI is a derivative-free (48) optimization method for parametric estimation $\boldsymbol{\theta}$, based on ensemble Kalman filtering (EnKF) (54), which is used for estimating states $\boldsymbol{z}(t)$ in numerical weather prediction (NWP) (55) given noisy observations. EKI (56) attempts to find a distribution of model parameters $\boldsymbol{\theta}$ that can describe time-averaged statistics of a truth, which could be from observational data or simulations, removing dependence on state variables by utilizing long integrations. EKI optimizes for macrophysical climate statistics (e.g., derived by averaging over many occurrences of the event of interest).

Quantification of parametric uncertainty is important as it illustrates how perturbations of parameters $\boldsymbol{\theta}$ that we want to estimate would translate to the predictions of $\boldsymbol{z}$. As shown in **Figure 2*e***, though an optimal value of $\boldsymbol{\theta}^*$ minimizing the cost function only captures one prediction $\boldsymbol{z}(\boldsymbol{\theta}^*)$, a range of $\boldsymbol{\theta}$ could yield wide-ranging predictions (e.g., covering extreme events). Running ensembles of forward physics-based simulations $\boldsymbol{f}(\boldsymbol{\theta})$ with a range of $\boldsymbol{\theta}$ for climate models to quantify these uncertainties propagated by parameter uncertainty is currently computationally infeasible. To address this challenge, the calibrate-emulate-sample (CES) approach (49, 50) trained

Review in Advance. Changes may still occur before final publication.

Downloaded from www.annualreviews.org. University of Chicago Libraries (ar-129425) IP: 128.135.43.97 On: Tue, 03 Dec 2024 18:25:25

INVERSE PROBLEM AND DATA ASSIMILATION

The problems of estimating parameters $\boldsymbol{\theta}$ and states $\boldsymbol{z}$ of a model $\boldsymbol{f}(\boldsymbol{z}, \boldsymbol{\theta})$ falls under the umbrella of inverse problems (60). The importance of parametric and state estimations lies in the fact that direct observations of model parameters and states are often unavailable, yet they are crucial for simulating and predicting both the weather and climate accurately. Various inverse problems arise in weather and climate, such as estimating parameters in climate models or determining initial conditions for improved weather forecasting. Data assimilation (61) refers to the process of combining observational data with numerical models. The synergies between data assimilation and ML have been increasingly recognized (62–64), including using ML to correct model error in data assimilation (65) and emulation of a dynamical system (66).

a GPR (Gaussian process regression) as a cheap method to emulate the prediction of interest $\boldsymbol{z}$ as a function of θ. Sampling the GPR emulator with Markov chain Monte Carlo enables substantially faster UQ (uncertainty quantification) of the predictions $\boldsymbol{z}$ resulting from the plausible range of $\boldsymbol{\theta}$. GPR has also been used directly for calibrating parameters with UQ in Earth system models (57).

2.2.4.2. Physics-informed neural networks (PINNs). The use of PINNs (58, 59) for planetary-scale geophysical flow problems has started to emerge in the past few years. Introduced by Raissi et al. (58), a PINN is a differentiable solver for partial differential equations (PDEs) that is particularly useful for inverse problems involving sparse-data inference, superresolution, data denoising, and state estimation $\boldsymbol{z}$ in data assimilation (see the sidebar titled Inverse Problem and Data Assimilation). Unlike classical ML in which the cost function typically only involves data, PINN encodes physics-based equations directly in the cost function (**Figure 3*a***).

Throughout the training iterations, the optimizer identifies the best ML-parameterized states $\boldsymbol{z} = NN(\boldsymbol{x}, t, \boldsymbol{\gamma})$ that are consistent with both the data and the governing equations. In the small-data regime, without evaluating the NN-parameterized $\boldsymbol{z}$ against known physical laws (such as conservation of mass, momentum, and energy), the ML predictions can be physically inconsistent and nonextrapolatable beyond the available observational data (e.g., deviation from truth in **Figure 2*g***). In contrast, by incorporating PDEs, PINNs can achieve both physics-informed data interpolation and extrapolation, as demonstrated by the examples in **Figure 3**, which cannot be achieved by ML models trained with observational data alone.

Figure 3*b*,*c* demonstrate the applications of PINNs on observations, ranging from estimating the initial conditions $\boldsymbol{z}(\boldsymbol{x}, t = 0)$ of hurricanes for subsequent forecasts (67) to inferring the nonmeasurable viscosity structure $\boldsymbol{z}(\boldsymbol{x})$ of Antarctic ice shelves (68). Both examples fall within the small-data regime in the upper left corner of **Figure 1*a***, where incorporating knowledge of PDEs becomes crucial for solving the inverse problems; the PINN-reconstructed wind field $\boldsymbol{z}(\boldsymbol{x}, t)$ (**Figure 3*b***) involves only sparse observations of wind velocity itself as training data, obtained from measurements by hurricane hunter planes and dropsondes. The PINN prediction of ice viscosity is achieved without any observations of viscosity in the training data (**Figure 3*c***); it relies solely on equations and other observable states (velocity and thickness fields) as training data. Thus, both examples involve substantial extrapolation beyond the sparse observational data, i.e., limited velocity data and no viscosity data.

As long as the same data and physics-based equations are used to solve the inverse problem, the predictions generated by properly trained PINNs are as trustworthy as those produced by established data assimilation methods. Due to PINN's leverage of a graphics processing unit (GPU) and differentiable modeling to infer accurate initial conditions without ensembles of forward modeling, as used in ensemble-based data assimilation methods (67) (see **Supplemental Text, Section I**

Review in Advance. Changes may still occur before final publication.

Downloaded from www.annualreviews.org. University of Chicago Libraries (ar-129425) IP: 128.135.43.97 On: Tue, 03 Dec 2024 18:25:25

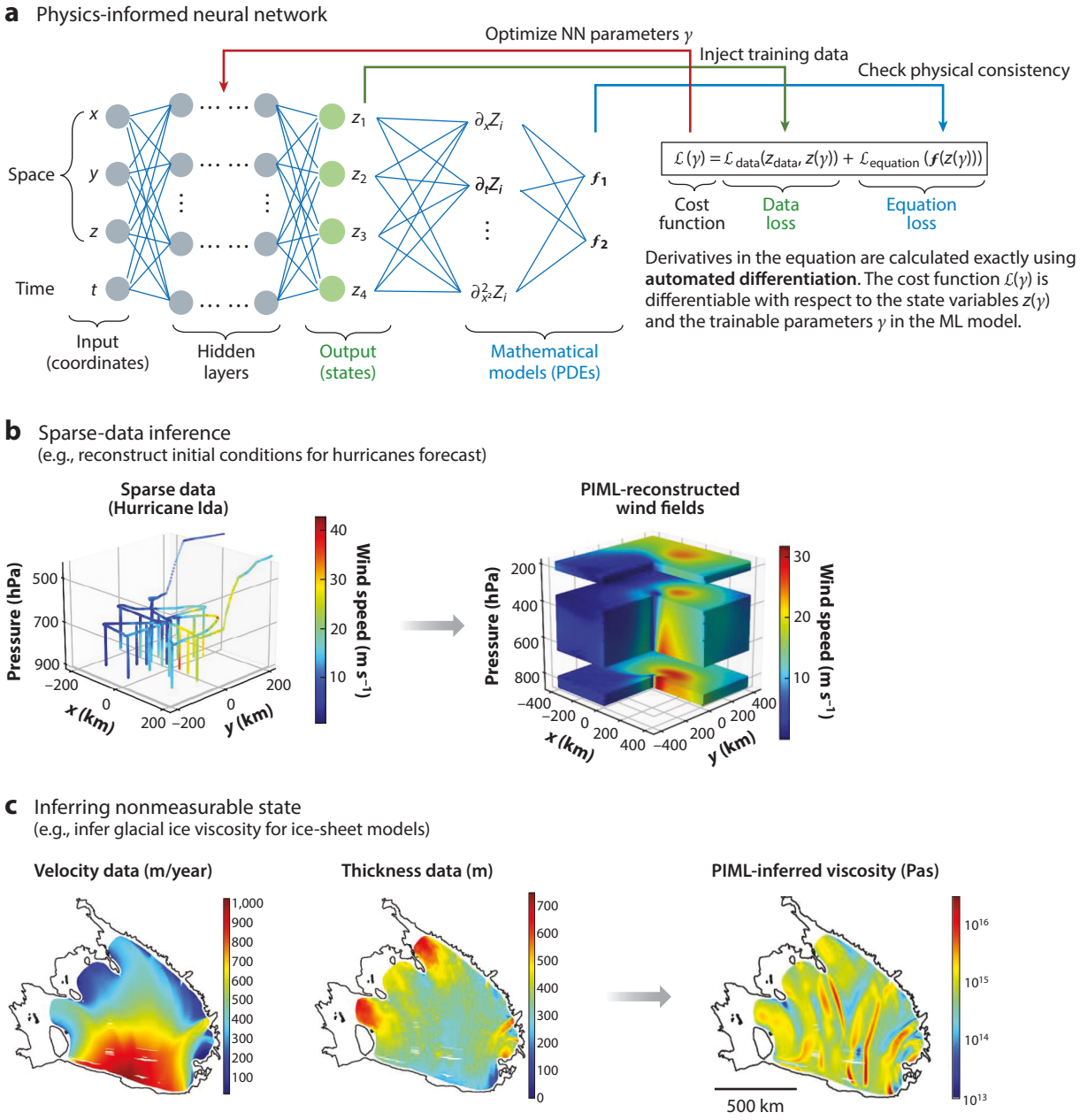

Figure 3

(*a*) The PIML algorithm and its applications in data assimilation (*b*,*c*). Panels *b* and *c* adapted with permission from Reference 67 (CC BY 4.0) and Reference 68 (CC BY 4.0), respectively. Abbreviations: ML, machine learning; NN, neural network; PDE, partial differential equation; PIML, physics-informed machine learning.

Review in Advance. Changes may still occur before final publication.

Downloaded from www.annualreviews.org. University of Chicago Libraries (ar-129425) IP: 128.135.43.97 On: Tue, 03 Dec 2024 18:25:25

for a brief comparison), PINNs require fewer computational resources to construct hurricane initial conditions with similar accuracy as the ensemble-based data assimilation methods (69). That being said, established data assimilation methods are supported by several mature theories, which are relatively lacking for PINN methods. Although several models used in climate predictions are not easily differentiable without substantial engineering efforts, the development of differentiable solvers for atmospheric dynamics (70) demonstrates promises. Differentiable ice-flow solver and emulator have also recently emerged as new tools for forward and inverse ice-flow modeling (71).

2.2.4.3. Equation discovery. Existing equations $\boldsymbol{f}(\boldsymbol{z}, \boldsymbol{\theta})$ describing the numerous processes in the climate system, particularly the SGS processes, are far from complete. Equation discovery, which outputs equations that are most consistent with data, has been used to tackle this problem. Inspired by earlier symbolic regression algorithms for distilling physical laws from data (72), sparse identification of nonlinear dynamics (SINDy) (73) has emerged as a widely used method for discovering $\boldsymbol{f}(\boldsymbol{z}, \boldsymbol{\theta})$ from data of the states $\boldsymbol{z}(t)$. It demonstrates the power of sparse regression for learning the most relevant terms in the prescribed function library that describes the data. To learn the correct $\boldsymbol{f}(\boldsymbol{z}, \boldsymbol{\theta})$, SINDy requires sampled data of both $\boldsymbol{z}(t)$ and $\mathrm{d}\boldsymbol{z}(t)/\mathrm{d}t$. For many climate problems these state measurements are sparse and noisy, or entirely unavailable. Schneider et al. (74) showed that time-averaged statistics of the states $\boldsymbol{z}(t)$, which are available for the climate system, can be sufficient to recover both the functional form of $\boldsymbol{f}(\boldsymbol{z}, \boldsymbol{\theta})$ and the noise level of the data using sparse regression combined with EKI. Sparse EKI is robust to noisy data and was successfully implemented to recover the Lorenz 96 equations (74). Other approaches for equation discovery from data assimilation increments (75, 76) and from partial observations (77), motivated by climate problems, have been proposed too.

Arguably the most successful example of the application of equation discovery for climate physics so far has been the learning of an ocean mesoscale SGS parameterization (78). Trained on high-resolution simulation data, Zanna & Bolton (78) showed that Bayesian linear sparse regression with relevance vector machines identifies relevant terms in the prescribed function library to discover the closed-form equations of $\Pi(\bar{z})$ (defined in **Figure 2**) for eddy momentum and temperature forcing. The closed-form equation is consistent with an analytically derivable physics-based model (79, 80). As discussed later in Section 3.1, SGS parameterizations (**Figure 2**) are essential for improving the accuracy of computationally feasible low-resolution climate simulations. Although black-box NNs have also shown promise for developing data-driven SGS parameterizations (Section 3.1), the significant interest in equation discovery stems from their better generalization to future climates and their interpretability (*upper side* of **Figure 1*b***).

Inspired by early work on symbolic regression (72, 81), the symbolic genetic algorithm (82) was developed to discover PDEs without the need to predetermine a function library. It uses a binary tree to parameterize common mathematical operations (e.g., addition, multiplication, derivative, division) and finds the correct operations such that the discovered equation matches the data. In climate applications, genetic algorithms have been used for finding equations for cloud cover parameterization (83) and ocean parameterization (84).

3. MACHINE LEARNING FOR CLIMATE SIMULATIONS

We discuss two major directions leveraging ML methods to improve the accuracy of climate simulations: (*a*) SGS parameterization, aimed at developing more accurate climate models via better representation of small-scale (expensive to resolve) physical processes, and (*b*) emulators, aimed at generating large ensembles of simulations (or directly, the statistics) at a fraction of the computational cost of a physics-based climate simulation. These two approaches are briefly discussed below.

Review in Advance. Changes may still occur before final publication.

Downloaded from www.annualreviews.org. University of Chicago Libraries (ar-129425) IP: 128.135.43.97 On: Tue, 03 Dec 2024 18:25:25

UNCERTAINTIES IN CLIMATE PROJECTIONS

Climate projections are affected by three sources of uncertainty (86): (*a*) model uncertainty (also known as structural error), (*b*) internal variability uncertainty (e.g., the signal-to-noise ratio problem), and (*c*) scenario uncertainty (related to how much greenhouse gases will be released in the future). Reducing model uncertainty requires developing more accurate climate models (e.g., improving parameterization or increasing resolutions), whereas reducing the internal variability uncertainty and scenario uncertainty requires computationally efficient climate models that can generate long, large ensembles of simulations and explore different scenarios.

3.1. Subgrid-Scale Parameterization

There are two reasons climate models require SGS parameterization to achieve simulations on relevant century-long timescales: (*a*) the process of interest varies on length scales or timescales smaller than a climate model's resolution, and (*b*) equations to describe the process are not known. SGS parameterizations estimate the effect of these unresolved processes on the resolved scales. Developing SGS parameterizations for climate modeling, but also for high-resolution simulations in limited domain, has been an active area of research since the pioneering work of Smagorinsky (85) on the first climate models in the early 1960s. Still, the approximations made in formulating these parameterizations remain a leading cause of model uncertainty (also known as structural error; see the sidebar titled Uncertainties in Climate Projections). ML presents a potentially exciting path forward in improving these SGS parameterizations or developing new ones. The general idea is to use observations or high-resolution simulations to learn a data-driven representation or closed-form equation of the SGS term Π (defined in **Figure 2**). Examples of the latter approach were discussed in Section 2.2.4; below, we mainly focus on approaches based on NNs (**Figure 2*j***).

Studies have demonstrated the ability of ML algorithms such as NNs to learn ML-based parameterizations as a supervised learning task, $NN(\bar{\boldsymbol{z}}, \boldsymbol{\gamma}) = \Pi(\bar{\boldsymbol{z}})$, for prototypes of geophysical turbulence (e.g., 78, 87), ocean turbulence (e.g., 88, 89), moist convection and clouds (e.g., 90–96), and atmospheric gravity waves (e.g., 97–99). Some of these examples have achieved stable simulations that are more accurate than simulations with traditional physics-based parameterizations (e.g., 78, 87, 93, 95). However, though promising, this approach faces a number of challenges. Some are common among other ML applications to climate (e.g., interpretability, extrapolation) and are discussed in Section 4. Challenges specific to SGS parameterization via supervised learning include availability of suitable high-resolution training data from numerical studies or observational campaigns, as well as issues with accuracy and stability once these ML-based SGS parameterizations are coupled [e.g., with atmosphere (93, 100) and ocean models (78)].

This discussion of SGS parameterization for climate models would not be complete if we did not emphasize the distinct challenges compared to its use in weather forecasting. In weather forecasting, the objective is to predict a specific trajectory based on initial conditions, necessitating accurate and detailed prediction of SGS physics. Conversely, climate studies aim to predict changes in the system's average behavior over decades. Thus, it is sufficient to predict the SGS statistics rather than all its specific features. This shift requires novel ML approaches optimized to capture emergent statistics rather than detailed information from training data in supervised learning. This poses challenges, as long term observations of climate statistics are limited and the simulations coupled with ML-based SGS parameterizations need to be stable for a long enough timescale to learn the climate statistics from the training data. Despite these challenges, a few studies have made progress in producing stable and accurate simulations of simple climate

Model uncertainty: deviation of the physics-based model from the data, due to inaccurate parameters θ or the physics equations f itself

Structural error: a type of model uncertainty arising from inaccuracies in the equations used to represent the data or processes of interest

ML-based SGS parameterization: SGS parameterization represented by an ML model rather than physics-based equations

Review in Advance. Changes may still occur before final publication.

Downloaded from www.annualreviews.org. University of Chicago Libraries (ar-129425) IP: 128.135.43.97 On: Tue, 03 Dec 2024 18:25:25

prototypes using NNs trained with differentiable modeling (101) and EKI (100) that target the evolution of the climate variables in response to the SGS processes rather than training on the SGS processes themselves. Recently, Google Research has made strides in this direction by developing an atmospheric model's dynamical core that learns SGS physics statistics directly from reanalysis data (70). Yet, numerical stability and satisfaction of global energy conservation constraints remain a challenge. Unlike in the weather literature, training from direct observations (102) has not been attempted yet, possibly because of the sparsity of global datasets with long enough timescales to capture climate statistics.

An additional challenge is how to address the interactions between different SGS processes, for example, between SGS parameterizations of ocean and atmosphere boundary layer turbulence that interact through air–sea fluxes. Training is typically done on subcomponents of the full climate system because it is not computationally feasible to run global climate simulations that fully resolve all SGS processes and their interactions. Concurrent observations of different SGS processes are also limited. As a result, interactions among a number of individually trained/calibrated data-driven parameterizations can lead to inaccurate or even unstable global simulations. This is an area in need of practical advancements.

Spatiotemporal emulator: an emulator with predictions that evolve with space and time

Initial value problem: a forward model $\boldsymbol{f}(\boldsymbol{z})$ with predictions $\boldsymbol{z}(t)$ subject to the initial conditions $\boldsymbol{z}(t_0)$ specified at time t_0

Boundary value problem: a forward model $\boldsymbol{f}(\boldsymbol{z})$ with predictions $\boldsymbol{z}(t)$ subject to the boundary conditions $\boldsymbol{z}(x_0, t)$, which can be time-evolving, at the boundaries x_0

3.2. Climate Emulators

"Emulator" refers to several types of tools in the climate science literature. In general, an emulator is trained to mimic the data, from physics-based simulations or observations, to substantially reduce the computational cost of producing new climate predictions, e.g., for other climate conditions within the distribution of the training data.

Emulators can be used to interpolate the projections from expensive climate simulations, making their projections among different emission scenarios accessible without rerunning the simulations. Earlier use of ML for emulators followed the successful approach of traditional pattern-scaling emulators (103, 104), which, for example, predict the change in statistics of variables of interest (e.g., regional annual-mean surface temperature or the return period of extreme events at a later time) given a small set of inputs (e.g., year, greenhouse gas forcing, global mean surface temperature). Using ML techniques (e.g., GPR, NN), emulators such as ClimateBench (105) have been employed to estimate the climate impacts of anthropogenic emissions annually up to 2100. However, it remains to be demonstrated that their skill is superior to that of pattern-scaling emulators, i.e., emulators that regress regional temperature on global mean temperature or cumulative emissions.

Although the aforementioned emulators can predict aggregated statistics within an often large window of length scales and timescales, another type of emulator has emerged in recent years with the aim of predicting the evolution of the climate system at fine spatiotemporal scales. These spatiotemporal emulators leverage the success of ML-based weather forecast models, which are physics free and trained solely on reanalysis data (106) (spanning 1979-present; see the sidebar titled Reanalysis). Recent ML-based weather forecast models [e.g., FourCastNet (2), Pangu (3), GraphCast (4)] are time-stepping algorithms that solve the initial value problem of predicting the state $\boldsymbol{z}(t)$ of the global atmosphere forward in time (from t_i to t_{i+1}, then from t_{i+1} to t_{i+2}, and so on; **Figure 2*i***). They exhibit comparable or even better skill than the best physics-based weather prediction models for lead times of up to around 10 days (4). However, weather and climate predictions are different problems. The former is an initial value problem, whereas the latter is more akin to a boundary value problem in the sense that the focus is on how external boundary conditions impact the system over longer periods of time.

Review in Advance. Changes may still occur before final publication.

Downloaded from www.annualreviews.org. University of Chicago Libraries (ar-129425) IP: 128.135.43.97 On: Tue, 03 Dec 2024 18:25:25

REANALYSIS

Reanalysis, sometimes referred to as maps without gaps, refers to a method of using a physical model to assimilate disparate observational data streams into a combined multivariate dataset uniform in space and time. The model fills in the data-poor regions and ensures physical consistency between variables. The output is often referred to as reanalysis data; however, it is important to keep in mind that these data are not observations but outputs of a forecast model. In fact, reanalysis products from different weather centers usually differ among themselves, and this spread can be taken as a measure of uncertainty in observations and understanding.

For climate predictions, atmospheric spatiotemporal emulators are built to solve boundary value problems that integrate the global atmospheric state given external forcings (e.g., radiative forcing) and time-evolving boundary conditions (e.g., sea-surface and land temperature) for decades or centuries. The AI2 Climate Emulator (ACE) (10, 11) is a promising example of such a spatiotemporal emulator trained on physics-based simulations. Similar work on oceanic spatiotemporal emulators (107, 108) suggests that coupled climate emulators might start to emerge as well.

ML spatiotemporal emulators have shown even more promise in simulating components of the climate system whose physics are less well understood. For the cryosphere, deep learning-based emulators for seasonal sea ice prediction have been found to outperform state-of-the-art physics-based dynamical models in terms of forecast accuracy (109–111), with a lead time of a few months. Some of these sea ice emulators capture atmospheric-ice-ocean interactions by training with appropriate climate variables (109, 111). Because these emulators were trained directly on sea ice observational data, they learn the atmospheric-ice-ocean interactions that are incompletely parameterized in the physics-based dynamical models, thereby correcting the model's structural error.

3.3. Physics-Informed Machine Learning (PIML)

Despite ML's ability to emulate weather (Section 3.2) and parameterize SGS processes when trained on high-resolution simulations or observations (Section 3.1), there is no guarantee that its predictions are physically sound (e.g., conservation of mass, energy). This physical inconsistency is problematic and makes long-term climate projections using ML-based emulators and ML-based parameterizations not trustworthy (**Figure 2*g***, *left panel*; see the sidebar titled Challenges and Opportunities of ML-Based Emulators). Incorporating physics constraints such as conservation laws, symmetries, and more broadly, equivariances (defined below), has been shown to alleviate a number of challenges such as instabilities and learning in the small-data regime—Kashinath et al. (114) review earlier work in PIML for weather and climate modeling.

3.3.1. Conservation laws. Various methods exist for incorporating conservation laws into ML models, such as embedding them in the loss function [e.g., PINNs (58); Section 2.2.4.2] or other components of the ML architecture. For instance, Beucler et al. (115) demonstrated that conserving quantities like mass and energy can be enforced as hard constraints within the NN architecture. Their architecture-constrained NN, trained as an SGS parameterization of moist convection, significantly improved simulated climate.

3.3.2. Symmetries and equivariances. Incorporating symmetries and equivariances has also shown advantages, particularly in the small-data regime. For a variable x, the nonlinear function g is equivariant under transformation $\mathbf{A}$ if $\mathbf{A}g(x) = g(\mathbf{A}x)$. For example, by incorporating various symmetries (e.g., scale equivariance, rotational equivariance) into convolutional neural networks (CNNs) trained on turbulence data from previous time steps, the CNNs generalize well to future

Review in Advance. Changes may still occur before final publication.

Downloaded from www.annualreviews.org. University of Chicago Libraries (ar-129425) IP: 128.135.43.97 On: Tue, 03 Dec 2024 18:25:25

CHALLENGES AND OPPORTUNITIES OF MACHINE LEARNING–BASED EMULATORS

Emulators can address the climate response to a particular emission scenario and internal variability uncertainty (defined in the sidebar titled Uncertainties in Climate Projections). However, emulators are at best as accurate as the data they are trained on, which may still contain model uncertainty; this may be partially overcome by training with data from very high-resolution yet very expensive simulations, such as the emerging global 1-km climate simulations. Nonetheless, major questions about the stability and physical consistency of the trained spatiotemporal emulators need to be addressed. For example, ML weather forecast models have been shown to produce unstable or unphysical atmospheric circulations beyond 10 days, poorly represent small-scale processes (15, 112), and fail to reproduce the chaotic behavior of weather (113). Potential solutions to address these challenges include incorporating physical constraints into ML models (Section 3.3) and developing a deeper understanding of the different sources of error in these models (Sections 4.1 and 4.2).

time steps (8) (**Figure 2*b***). Enforcing rotational equivariance through Capsule NN, CNNs, or customized latent spaces has improved ML-based predictions of large-scale weather patterns (116) and turbulent flows (8, 117).

3.3.3. Spectrum information. Including information about the Fourier spectrum of geophysical turbulence in the loss function has been shown to aid in learning small scales and reducing spectral bias, thereby improving the stability and physical consistency of ML-based emulators (112). See Section 4.1 for further discussions.

4. CHALLENGES AND PROMISES

4.1. Quantifying Uncertainties of Machine Learning Models

Broadly speaking, there are two sources of error in ML-based models: errors in the training data and the epistemic uncertainty for the ML model. The errors in data can stem from sparsity and measurement noise, which are particularly relevant for observations, or from errors in simulation data, which can arise from numerical errors and inaccurate physics-based equations. The epistemic uncertainty of the ML model arises from different sources, such as model architecture and hyperparameters (118). Some ML techniques, such as GPR, provide rigorous estimates of uncertainty (see, e.g., References 26 and 105 for climate applications). However, for deep learning, UQ (uncertainty quantification) is more complicated and the subject of extensive research (for recent review papers in the context of scientific applications see References 118 and 119).

Spectral bias: neural networks' tendency to preferentially capture certain frequencies of the training data

Epistemic uncertainty: deviation of the ML model from the data, can be due to approximation, optimization, and generalization errors

Understanding the sources of errors in ML models can improve their stability, physical consistency, and reliability. For example, in simulations coupled with ML-based parameterization, errors from the ML model are propagated into the simulations and vice versa, potentially leading to instabilities and nonphysical behavior. Similarly, errors in a spatiotemporal emulator can accumulate and destabilize the emulation. Because we cannot directly estimate accuracy during inference (as we do not have access to the ground truth), the best approach is to estimate the uncertainty of the ML model's output, as this uncertainty may be indicative of its accuracy. Here, we provide examples from climate science for UQ of NNs, and we also discuss two impactful sources of epistemic uncertainties related to representation error (e.g., spectral bias) and data imbalance (e.g., rare extreme events).

4.1.1. Quantifying epistemic uncertainty. A variety of techniques from the ML literature have been employed for UQ of NNs in climate applications. For instance, deep ensembles (24,

Review in Advance. Changes may still occur before final publication.

Downloaded from www.annualreviews.org. University of Chicago Libraries (ar-129425) IP: 128.135.43.97 On: Tue, 03 Dec 2024 18:25:25

120–122) and Bayesian NNs (24, 123) are used to assess the mean and spread of predictions as well as the faithfulness of the NN optimization. In Reference 124, these two methodologies were combined to reveal the consequences of architecture choice, as determined by UQ and the ability to approximate the physical system. Other techniques, such as variational autoencoders, dropout, and abstention, have also been explored (123, 125–127). See References 128 and 123 for detailed discussions.

Climate-invariant machine learning: machine learning that utilizes relationships that stay the same across different climates to improve generalization

4.1.2. Spectral bias. Another example of epistemic error in ML models affecting climate applications is the spectral bias (129) (or frequency principle; 130). Namely, NNs learn to represent the large scales much more easily than small scales, which can pose challenges for multiscale climate problems. **Figure 4*a*** shows the spectrum of the one-time-step (∼6 or 12 h) prediction of upper-level wind from a few state-of-the-art ML weather emulators. Although the predictions exhibit the correct spectrum for up to zonal Fourier wave numbers of ∼30 (scales of 40,000 km to 500 km), smaller scales (from 500 km to 25 km) are poorly learned. It's noteworthy that these predictions all boast around ∼99% accuracy based on anomaly pattern correlation. These errors in small scales grow to larger scales after 10 days. Eventually, these predictions either blow up or become unphysical (112). The same behavior is observed in simpler tasks such as reconstruction of atmospheric boundary layer turbulence (**Figure 4*b***), time-stepping prediction for quasigeostrophic (QG) turbulence (**Figure 4*c***) and its reconstruction (**Figure 4*d***), or even a simple 1D function (**Figure 4*f***). Promising solutions include Fourier regularization of the loss function (**Figure 4*c***, modified from Reference 112) and random Fourier features (134, 135) (**Figure 4*d***, modified from Reference 76). Superposing small NNs (132, 133) via the multistage NNs also improves spectral bias substantially compared with vanilla NNs (**Figure 4*e***, modified from Reference 132).

4.1.3. Rare extreme events. Another example of epistemic error relates to rare events (e.g., heat waves, hurricanes, ice-shelf collapse, ocean circulation collapse). Predicting these rare events is crucial, but they are often underrepresented or entirely absent from the training set, leading to significant data imbalance. Addressing data imbalance and improving the learning of rare events is an active area of research. Common approaches such as resampling (136, 137), using weighted loss function (123, 138), and learning the causal relationship that drives the rare behavior (124) have shown promise. Innovative approaches, such as combining ML-based emulators with mathematical tools for rare events (139, 140), may enable the learning of the rarest events.

4.2. Nonstationarity: Out-of-Distribution Error of Machine Learning Models

Climate change is inherently nonstationary (28): The mean state and its variability change over time. This poses a major challenge for applications of ML models to climate-change projections. For instance, ML-based models trained on data from the current climate may not perform well for a warmer future climate with higher greenhouse gas concentrations. Studies have already demonstrated unstable or unphysical simulations resulting from NN's inability to extrapolate beyond its training data (93, 141, 142). The nonstationary problem raises new questions: How can we ensure that the prediction task is within the distribution of the training data? How do we ensure that the ML model leverages information that is climate-invariant? Would a hybrid approach, coupling physics- and ML-based models, improve long-term climate simulations?

Examples of strategies for dealing with nonstationarity and out-of-distribution generalization include (*a*) incorporating physical knowledge (142) and (*b*) transfer learning (87, 141). As an example of incorporating physical knowledge, the recently proposed climate-invariant machine learning (142) learns the mapping between variables of interests that is universal across climates.

Review in Advance. Changes may still occur before final publication.

Downloaded from www.annualreviews.org. University of Chicago Libraries (ar-129425) IP: 128.135.43.97 On: Tue, 03 Dec 2024 18:25:25

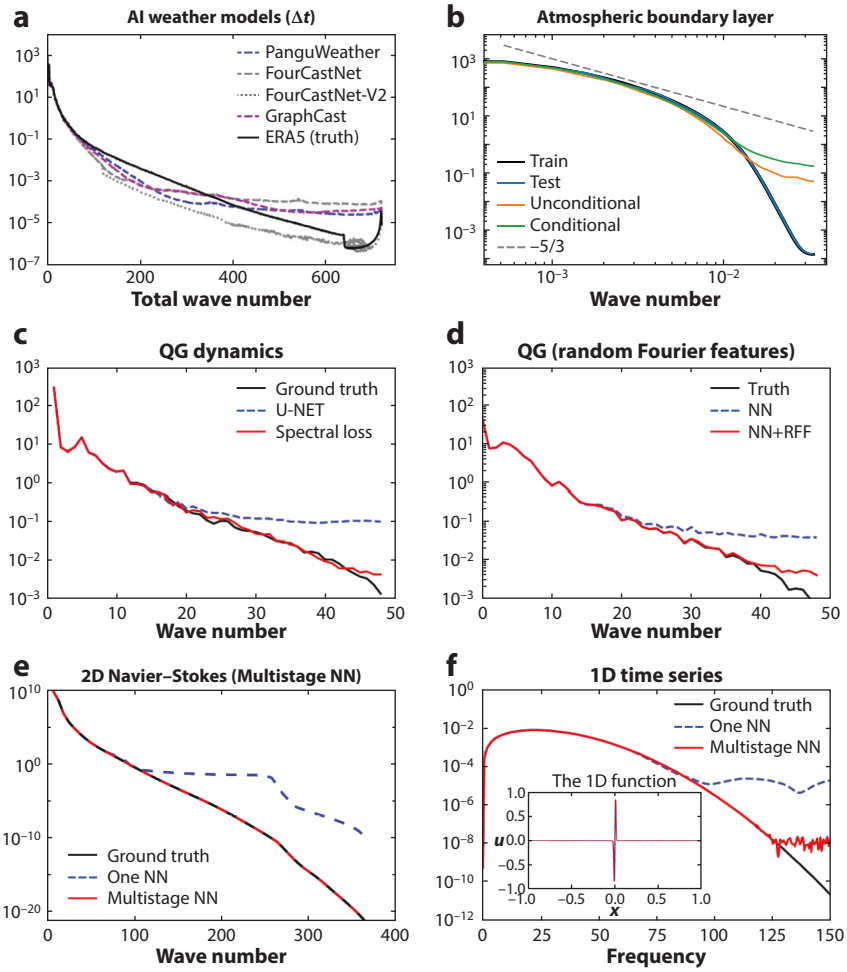

Figure 4

The spectral bias of neural networks (129, 130) can be widely observed in climate applications and can cause major challenges such as instabilities. (*a*) State-of-the-art ML-based weather emulator predictions after one time step (based on results from Reference 112, courtesy of Qiang Sun). (*b*) Atmospheric boundary layer turbulence reconstruction (131). (*c*,*d*) QG turbulence prediction after one time step (112) (data provided by Ashesh Chattopadhyay) or reconstruction (based on results from Reference 76, data provided by Rambod Mojgani). (*e*) Reconstruction of a 2D flow field (132) using the multistage NN (133). (*f*) Reconstruction of a 1D function with sharp peaks, difficult to fit with vanilla NNs (data provided by Yongji Wang). Panels *a*, *b*, and *e* adapted with permission from Reference 112 (CC BY 4.0), Reference 131 (CC BY 4.0), and Reference 132 (CC BY 4.0), respectively. Panels *c* and *d* adapted with permission from Reference 76 (CC BY 4.0). Abbreviations: 1D, one-dimensional; 2D, two-dimensional; AI, artificial intelligence; ERA5, the 5th generation ECMWF atmospheric reanalysis of the global climate; ML, machine learning; NN, neural network; QG, quasigeostrophic; RFF, random Fourier feature.

This study showed promising offline results of data-driven parameterization of moist convection across a range of cold to warm climates once temperature, relative humidity, and latent heating were properly transformed. This approach leverages physical insights of climate. The main challenge is finding the appropriate transformations, which are easier to find for thermodynamics but harder to find for dynamics (e.g., wind).

Review in Advance. Changes may still occur before final publication.

Downloaded from www.annualreviews.org. University of Chicago Libraries (ar-129425) IP: 128.135.43.97 On: Tue, 03 Dec 2024 18:25:25

Transfer learning, which is a common framework in ML for addressing out-of-distribution generalization, involves training an ML model for a given system (e.g., the current climate) and then retraining it with a much smaller amount of data from a new system (e.g., a warmer climate). The retrained ML model could then perform better for the new system. Several studies have demonstrated the potential of transfer learning to address significant changes in parameters θ (e.g., a 100-times increase in Reynolds number in geophysical turbulence) or forcing (87, 141). The key challenge with transfer learning is obtaining reliable data for retraining. In climate-change prediction, we must rely on simulations, as observations from the future are unavailable. Libraries of high-resolution global and regional simulations that strategically sample from a range of climates are emerging, providing a valuable source of training and retraining data (143–145). However, the range of scenarios typically explored with Earth system models is typically restricted to plausible future scenarios. As ML techniques become more mainstream in climate studies, it will be important to simulate a wider range of future climates to expand the range of training data, especially in extreme regimes.

4.3. Understanding What Machine Learning is Learning

Understanding what an ML model has learned, and how and why, is essential for climate applications, especially to gain trust of and further improve such models. The use of explainable artificial intelligence (XAI) techniques from the ML community for climate applications has gained popularity in recent years (e.g., 120, 146–148). For review papers featuring XAI in climate science, see References 149–152. A core strategy for many XAI techniques is to identify which parts of the inputs of an NN (e.g., regions of the atmosphere or ocean) are used to predict a specific output. For example, Toms et al. (153) illustrated XAI could infer scientifically meaningful information regarding climate patterns known as El Niño events. In Labe & Barnes (154), XAI was used to assist model comparisons of the Arctic. XAI is also often used to determine whether the ML has gained skill through detecting meaningful patterns in the training data, instead of spurious correlations. Sonnewald et al. (120) used XAI within an ensemble of NNs to determine their ML model's accuracy (**Figure 5***a*,*b*) by assessing conformance with theory. The ML model's task was to predict ocean physical regimes, i.e., dominant balances between terms in the equation governing the flow. Similar equation-determining frameworks are in References 24, 121, and 124.

Standard techniques for analyzing physical systems can also be applied to understand NNs. For example, Fourier analysis has provided insight into NNs' learning process (129, 130). In the context of data-driven modeling of geophysical turbulence (141), Fourier analyses of CNNs revealed what they have learned. The convolution kernels (with over 1 million learnable parameters) were shown to fall into just a few classes: low- and high-pass filters, and Gabor wavelets (**Figure 5***c*). These findings align well with prior work that used wavelets for turbulence modeling (155), and even more so with theoretical ML studies on the need for such spectral filters for learning multiscale, localized data (156, 157). More recent work has found this approach useful in interpreting deep NNs in climate applications by examining concepts from physics and ML together (100, 112).

5. SUMMARY AND OUTLOOK

Numerous scientific discoveries and rigorous understandings have been prompted by first identifying empirical relationships. We summarized in Section 2.1 how ML can facilitate this, for example, by accelerating the search for patterns in climate data that can be used to derive physical understandings. We also summarized in Section 2.2 the promises ML has brought to find closed-form equations for poorly understood climate processes. In many aspects of the climate system,

Review in Advance. Changes may still occur before final publication.

Downloaded from www.annualreviews.org. University of Chicago Libraries (ar-129425) IP: 128.135.43.97 On: Tue, 03 Dec 2024 18:25:25

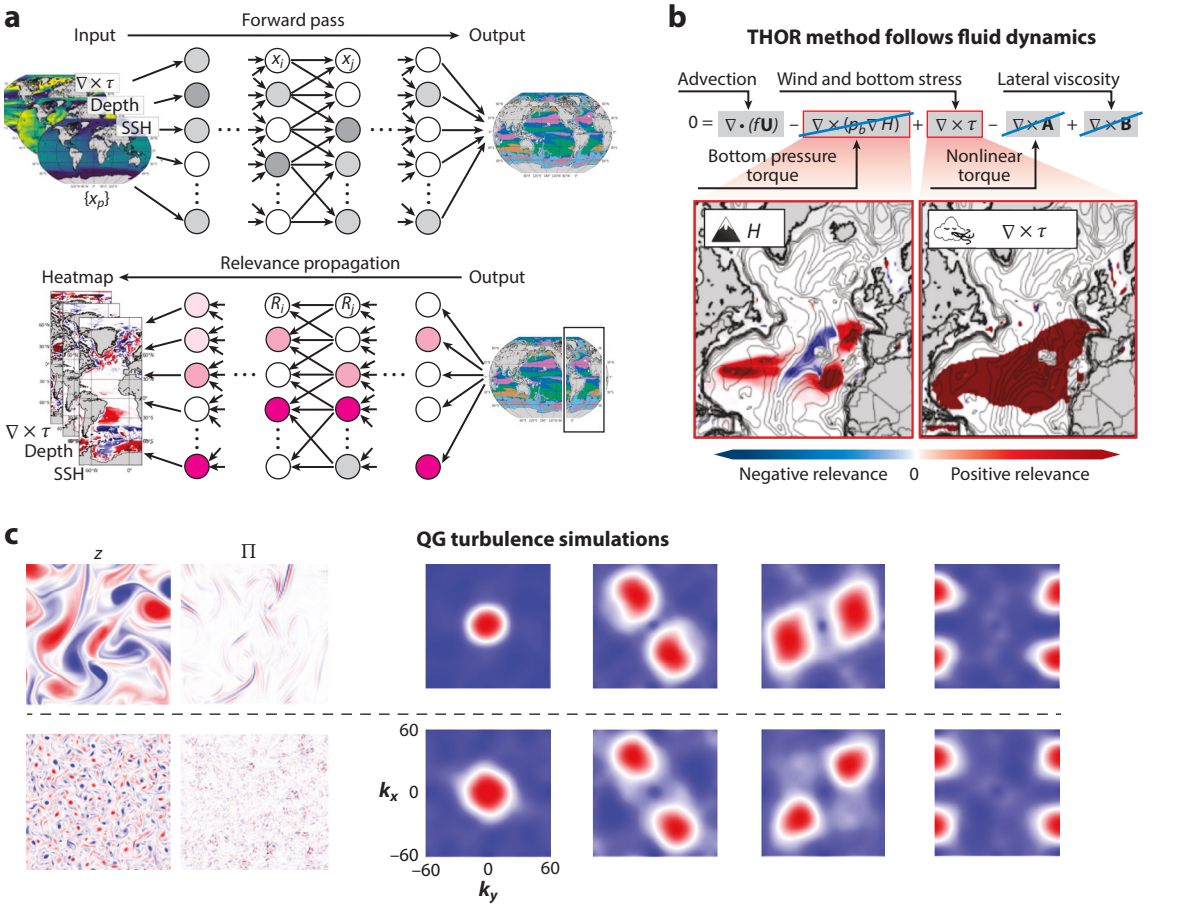

Figure 5

Understanding what ML learns. Panels *a* and *b* illustrate how the THOR method ensures the input data necessary for the ML model to demonstrate its learning of physics is present (120). (*a*, *top*) Training an NN to predict sections of the ocean dominated by different balances in equation terms describing the flow (*colors in output*) using related surface fields (e.g., wind). (*a*, *bottom*) Looking backward using XAI to see where in the input the NN saw as relevant (*blue*, not relevant; *red*, relevant). (*b*) For the pink section in the North Atlantic, only two equation terms are relevant (*red boxes*), and relevances show conformance in two maps below, e.g., where the mountain range (*closed black lines*) in depth (H) gives negative relevance. (*c*) The two leftmost panels show examples of the state $\mathbf{z}$ and SGS term Π (defined in **Figure 2**) from two setups of geophysical turbulence, separated by the dotted line, that differs in forcing scale and dynamics. The right-side panels show examples of the Fourier spectra of convolutional kernels of NNs trained as ML-based SGS parameterizations $NN(\bar{\mathbf{z}}, \gamma) = \Pi$. The Fourier analysis shows the emergence of low-pass, high-pass, and band-pass Gabor filters (141). Panels *a* and *b* adapted with permission from Reference 120 (CC BY 4.0). Panel *c* adapted with permission from Reference 141 (CC BY 4.0). Abbreviations: ML, machine learning; NN, neural network; QG, quasigeostrophic; SGS, subgrid-scale; SSH, sea surface height; THOR, Tracking global Heating with Ocean Regimes; XAI, explainable artificial intelligence.

we do not yet have accurate process-level models to describe the system (e.g., sea ice rheology and cloud microphysics). The increasing amount of observational data offers exciting opportunities for both equation and knowledge discovery to improve the fundamental understanding of climate physics.

However, ML can be used as tools to improve simulations. ML models can be coupled with traditional physics-based models and used to parameterize processes for which closed-form

Review in Advance. Changes may still occur before final publication.

Downloaded from www.annualreviews.org. University of Chicago Libraries (ar-129425) IP: 128.135.43.97 On: Tue, 03 Dec 2024 18:25:25

equations are not yet available (Section 3.1). ML has led to breakthroughs in weather forecasting, which was a task not widely expected to be possible a couple of years ago. We discussed the challenges scientists need to overcome when moving forward from weather forecasting to climate prediction (Sections 3.2 and 4).

ML is advancing rapidly, and new techniques and concepts that have shown great promise in other fields are now being quickly adopted in climate science. Notable examples, as of this writing, include diffusion models (e.g., citenprice2023gencast,bassetti2023diffesm,finn2024towards), LLMs (e.g., 160), and foundation models (see, e.g., Reference 161 for a discussion of their design and implementation and Reference 162 for a downstream task involving gravity waves). Progress in climate modeling could greatly benefit from collaborations among the ML, climate sciences, and mathematics communities. For example, the numerical analysis of differential equations and the advent of digital computers played a key role in starting the field of numerical weather and climate prediction (163). Developing similar rigorous tools, by closely combining methods from climate physics, ML theory, and numerical analysis, can potentially help with building stable, accurate, and trustworthy ML-based models.

DISCLOSURE STATEMENT

The authors are not aware of any affiliations, memberships, funding, or financial holdings that might be perceived as affecting the objectivity of this review.

ACKNOWLEDGMENTS

We thank Mingjing Tong, Oliver Dunbar, Jinlong Wu, and Duncan Watson-Parris for their helpful discussions regarding data assimilation methods, GPR with EKI, sparse learning, and emulators, respectively. We are grateful for the valuable general feedback from Andre Souza and Janni Yuval on this article. We also thank Qiang Sun, Ashesh Chattopadhyay, Rambod Mojgani, and Yongji Wang for helping to remake the spectral bias figure. C.-Y.L., R.F., P.H., and A.S. acknowledge the National Science Foundation for funding via grants DMS-2245228, AGS-2426087, OAC-2005123, and OAC-2004492, respectively. R.F., P.H., and A.S. also acknowledge funding from Schmidt Sciences through the Virtual Earth System Research Institute.

LITERATURE CITED

1. Keisler R. 2022. arXiv:2202.07575 [physics.ao-ph]
2. Pathak J, Subramanian S, Harrington P, Raja S, Chattopadhyay A, et al. 2022. arXiv:2202.11214 [physics.ao-ph]
3. Bi K, Xie L, Zhang H, Chen X, Gu X, Tian Q. 2023. *Nature* 619:533–38
4. Lam R, Sanchez-Gonzalez A, Willson M, Wirnsberger P, Fortunato M, et al. 2023. *Science* 382:1416–21
5. Chen L, Zhong X, Zhang F, Cheng Y, Xu Y, et al. 2023. *NPJ Clim. Atmos. Sci.* 6:190
6. Sonnewald M, Wunsch C, Heimbach P. 2019. *Earth Space Sci.* 6:784–94
7. Xiao Q, Balwada D, Jones CS, Herrero-González M, Smith KS, Abernathey R. 2023. *J. Adv. Model. Earth Syst.* 15:e2023MS003709
8. Wang R, Walters R, Yu R. 2021. Paper presented at the International Conference on Learning Representations (ICLR) 2021, Virtual Event, Austria, May 3–7
9. Yuval J, O'Gorman PA. 2020. *Nat. Commun.* 11:3295
10. Watt-Meyer O, Dresdner G, McGibbon J, Clark SK, Henn B, et al. 2023. arXiv:2310.02074 [physics.ao-ph]
11. Duncan JP, Wu E, Golaz JC, Caldwell PM, Watt-Meyer O, et al. 2024. *Mach. Learn. Comput.* 1(3):e2024JH000136
12. Hornik K, Stinchcombe M, White H. 1989. *Neural Netw.* 2:359–66

Review in Advance. Changes may still occur before final publication.

Downloaded from www.annualreviews.org. University of Chicago Libraries (ar-129425) IP: 128.135.43.97 On: Tue, 03 Dec 2024 18:25:25

13. Chen T, Chen H. 1995. *IEEE Trans. Neural Netw.* 6:911–17
14. Ravuri S, Lenc K, Willson M, Kangin D, Lam R, et al. 2021. *Nature* 597:672–77
15. Ben Bouallègue Z, Clare MC, Magnusson L, Gascon E, Maier-Gerber M, et al. 2024. *Bull. Am. Meteorol. Soc.* 105:E864–83
16. Ham YG, Kim JH, Luo JJ. 2019. *Nature* 573:568–72
17. Rasp S, Hoyer S, Merose A, Langmore I, Battaglia P, et al. 2024. *J. Adv. Model. Earth Syst.* 16:e2023MS004019
18. Pathak J, Hunt B, Girvan M, Lu Z, Ott E. 2018. *Phys. Rev. Lett.* 120:024102
19. Dueben PD, Bauer P. 2018. *Geosci. Model Dev.* 11:3999–4009
20. Weyn JA, Durran DR, Caruana R. 2019. *J. Adv. Model. Earth Syst.* 11:2680–93
21. Chattopadhyay A, Nabizadeh E, Hassanzadeh P. 2020. *J. Adv. Model. Earth Syst.* 12:e2019MS001958
22. Rasp S, Dueben PD, Scher S, Weyn JA, Mouatadid S, Thuerey N. 2020. *J. Adv. Model. Earth Syst.* 12:e2020MS002203
23. Rasp S, Thuerey N. 2021. *J. Adv. Model. Earth Syst.* 13:e2020MS002405
24. Clare MCA, Jamil O, Morcrette CJ. 2021. *Q. J. R. Meteorol. Soc.* 147:4337–57
25. Price I, Sanchez-Gonzalez A, Alet F, Ewalds T, El-Kadi A, et al. 2023. arXiv:2312.15796 [cs.LG]
26. Watson-Parris D. 2021. *Philos. Trans. R. Soc. A* 379:20200098
27. Schneider T, Behera S, Boccaletti G, Deser C, Emanuel K, et al. 2023. *Nat. Climate Change* 13:887–89
28. Palmer TN. 1999. *J. Climate* 12:575–91
29. Held IM. 2005. *Bull. Am. Meteorol. Soc.* 86:1609–14
30. Walker G. 1928. *Q. J. R. Meteorol. Soc.* :79–87
31. Corti S, Molteni F, Palmer T. 1999. *Nature* 398:799–802
32. Thompson DW, Solomon S. 2002. *Science* 296:895–99
33. Monahan AH, Fyfe JC, Ambaum MH, Stephenson DB, North GR. 2009. *J. Climate* 22:6501–14
34. Page J, Brenner MP, Kerswell RR. 2021. *Phys. Rev. Fluids* 6:034402
35. Lusch B, Kutz JN, Brunton SL. 2018. *Nat. Commun.* 9:4950
36. Shamekh S, Lamb KD, Huang Y, Gentine P. 2023. *PNAS* 120:e2216158120
37. Souza AN. 2023. arXiv:2304.03362 [physics.flu-dyn]
38. Geogdzhayev G, Souza AN, Ferrari R. 2024. *Phys. D Nonlinear Phenom.* 462:134107
39. Wang X, Slawinska J, Giannakis D. 2020. *Sci. Rep.* 10:2636
40. Rowley CW, Mezić I, Bagheri S, Schlatter P, Henningson DS. 2009. *J. Fluid Mech.* 641:115–27
41. Reichstein M, Camps-Valls G, Stevens B, Jung M, Denzler J, et al. 2019. *Nature* 566:195–204
42. Landy JC, Dawson GJ, Tsamados M, Bushuk M, Stroeve JC, et al. 2022. *Nature* 609:517–22
43. Martin SA, Manucharyan G, Klein P. 2024. *Geophys. Res. Lett.* 51(17):e2024GL110059
44. Rezvanbehbahani S, Stearns LA, Keramati R, Shankar S, van der Veen C. 2020. *Commun. Earth Environ.* 1:31
45. Surawy-Stepney T, Hogg AE, Cornford SL, Davison BJ. 2023. *Nat. Geosci.* 16:37–43
46. Lai CY, Kingslake J, Wearing MG, Chen PHC, Gentine P, et al. 2020. *Nature* 584:574–78
47. Lorenz EN. 1963. *J. Atmos. Sci.* 20:130–41
48. Iglesias MA, Law KJ, Stuart AM. 2013. *Inverse Probl.* 29:045001
49. Cleary E, Garbuno-Inigo A, Lan S, Schneider T, Stuart AM. 2021. *J. Comput. Phys.* 424:109716
50. Dunbar OR, Garbuno-Inigo A, Schneider T, Stuart AM. 2021. *J. Adv. Model. Earth Syst.* 13:e2020MS002454
51. Lopez-Gomez I, Christopoulos C, Langeland Ervik HL, Dunbar OR, Cohen Y, Schneider T. 2022. *J. Adv. Model. Earth Syst.* 14:e2022MS003105
52. Mansfield L, Sheshadri A. 2022. *J. Adv. Model. Earth Syst.* 14:e2022MS003245
53. Souza AN, Wagner G, Ramadhan A, Allen B, Churavy V, et al. 2020. *J. Adv. Model. Earth Syst.* 12:e2020MS002108
54. Evensen G. 1994. *J. Geophys. Res. Oceans* 99:10143–62
55. Houtekamer PL, Zhang F. 2016. *Mon. Weather Rev.* 144:4489–532
56. Kovachki NB, Stuart AM. 2019. *Inverse Probl.* 35:095005
57. Watson-Parris D, Williams A, Deaconu L, Stier P. 2021. *Geosci. Model Dev.* 14:7659–72

Review in Advance. Changes may still occur before final publication.

Downloaded from www.annualreviews.org. University of Chicago Libraries (ar-129425) IP: 128.135.43.97 On: Tue, 03 Dec 2024 18:25:25

58. Raissi M, Perdikaris P, Karniadakis GE. 2019. *J. Comput. Phys.* 378:686–707
59. Karniadakis GE, Kevrekidis IG, Lu L, Perdikaris P, Wang S, Yang L. 2021. *Nat. Rev. Phys.* 3:422–40
60. Tarantola A. 2005. *Inverse Problem Theory and Methods for Model Parameter Estimation*. Philadelphia: SIAM
61. Kalnay E. 2003. *Atmospheric Modeling, Data Assimilation and Predictability*. Cambridge, UK: Cambridge Univ. Press
62. Geer AJ. 2021. *Philos. Trans. R. Soc. A* 379:20200089
63. Brajard J, Carrassi A, Bocquet M, Bertino L. 2021. *Philos. Trans. R. Soc. A* 379:20200086
64. Cheng S, Quilodrán-Casas C, Ouala S, Farchi A, Liu C, et al. 2023. *IEEE/CAA J. Automat. Sin.* 10:1361–87
65. Farchi A, Laloyaux P, Bonavita M, Bocquet M. 2021. *Q. J. R. Meteorol. Soc.* 147:3067–84
66. Brajard J, Carrassi A, Bocquet M, Bertino L. 2020. *J. Comput. Sci.* 44:101171
67. Eusebi R, Vecchi GA, Lai CY, Tong M. 2024. *Commun. Earth Environ.* 5:8
68. Wang Y, Lai CY, Cowen-Breen C. 2022. **https://doi.org/10.21203/rs.3.rs-2135795/v1**
69. Lu X, Wang X, Tong M, Tallapragada V. 2017. *Mon. Weather Rev.* 145:4877–98
70. Kochkov D, Yuval J, Langmore I, Norgaard P, Smith J, et al. 2024. *Nature* 632:1060–66
71. Jouvet G, Cordonnier G. 2023. *J. Glaciol.* 2023:1–15
72. Schmidt M, Lipson H. 2009. *Science* 324:81–85
73. Brunton SL, Proctor JL, Kutz JN. 2016. *PNAS* 113:3932–37
74. Schneider T, Stuart AM, Wu JL. 2022. *J. Comput. Phys.* 470:111559
75. Lang M, Jan Van Leeuwen P, Browne P. 2016. *Tellus A Dyn. Meteorol. Oceanogr.* 68:29012
76. Mojgani R, Chattopadhyay A, Hassanzadeh P. 2024. *J. Adv. Model. Earth Syst.* 16(3):e2023MS004033
77. Chen N, Zhang Y. 2023. *Phys. D Nonlinear Phenom.* 449:133743
78. Zanna L, Bolton T. 2020. *Geophys. Res. Lett.* 47:e2020GL088376
79. Anstey JA, Zanna L. 2017. *Ocean Model.* 112:99–111
80. Jakhar K, Guan Y, Mojgani R, Chattopadhyay A, Hassanzadeh P. 2024. *J. Adv. Model. Earth Syst.* 16(7):e2023MS003874
81. Koza JR. 1994. *Stat. Comput.* 4:87–112
82. Chen Y, Luo Y, Liu Q, Xu H, Zhang D. 2022. *Phys. Rev. Res.* 4:023174
83. Grundner A, Beucler T, Gentine P, Eyring V. 2024. *J. Adv. Model. Earth Syst.* 16:e2023MS003763
84. Ross A, Li Z, Perezhogin P, Fernandez-Granda C, Zanna L. 2023. *J. Adv. Model. Earth Syst.* 15
85. Smagorinsky J. 1963. *Mon. Weather Rev.* 91:99–164
86. Hawkins E, Sutton R. 2009. *Bull. Am. Meteorol. Soc.* 90:1095–108
87. Guan Y, Chattopadhyay A, Subel A, Hassanzadeh P. 2022. *J. Comput. Phys.* 458:111090
88. Bolton T, Zanna L. 2019. *J. Adv. Model. Earth Syst.* 11:376–99
89. Sane A, Reichl BG, Adcroft A, Zanna L. 2023. *J. Adv. Model. Earth Syst.* 15:e2023MS003890
90. Gentine P, Pritchard M, Rasp S, Reinaudi G, Yacalis G. 2018. *Geophys. Res. Lett.* 45:5742–51
91. Gentine P, Eyring V, Beucler T. 2021. In *Deep Learning for the Earth Sciences: A Comprehensive Approach to Remote Sensing, Climate Science and Geosciences*, G Camps-Valls, D Tuia, XX Zhu, M Reichstein, pp. 307–14. Hoboken, NJ: Wiley
92. Yuval J, O'Gorman PA. 2023. *J. Adv. Model. Earth Syst.* 15:e2023MS003606
93. Rasp S, Pritchard MS, Gentine P. 2018. *PNAS* 115:9684–89
94. Grundner A, Beucler T, Gentine P, Iglesias-Suarez F, Giorgetta MA, Eyring V. 2022. *J. Adv. Model. Earth Syst.* 14:e2021MS002959
95. Arcomano T, Szunyogh I, Wikner A, Hunt BR, Ott E. 2023. *Geophys. Res. Lett.* 50:e2022GL102649
96. Watt-Meyer O, Brenowitz ND, Clark SK, Henn B, Kwa A, et al. 2024. *J. Adv. Model. Earth Syst.* 16:e2023MS003668
97. Matsuoka D, Watanabe S, Sato K, Kawazoe S, Yu W, Easterbrook S. 2020. *Geophys. Res. Lett.* 47:e2020GL089436
98. Espinosa ZI, Sheshadri A, Cain GR, Gerber EP, DallaSanta KJ. 2022. *Geophys. Res. Lett.* 49:e2022GL098174
99. Hardiman SC, Scaife AA, van Niekerk A, Prudden R, Owen A, et al. 2023. *Artif. Intel. Earth Syst.* 2:e220081

Review in Advance. Changes may still occur before final publication.

Downloaded from www.annualreviews.org. University of Chicago Libraries (ar-129425) IP: 128.135.43.97 On: Tue, 03 Dec 2024 18:25:25

100. Pahlavan HA, Hassanzadeh P, Alexander MJ. 2024. *Geophys. Res. Lett.* 51:e2023GL106324
101. Frezat H, Le Sommer J, Fablet R, Balarac G, Lguensat R. 2022. *J. Adv. Model. Earth Syst.* 14:e2022MS003124
102. McNally A, Lessig C, Lean P, Boucher E, Alexe M, et al. 2024. arXiv:2407.15586 [physics.ao-ph]
103. Beusch L, Gudmundsson L, Seneviratne SI. 2020. *Earth Syst. Dyn.* 11:139–59
104. Tebaldi C, Snyder A, Dorheim K. 2022. *Earth Syst. Dyn.* 13:1557–609
105. Watson-Parris D, Rao Y, Olivié D, Seland Ø, Nowack P, et al. 2022. *J. Adv. Model. Earth Syst.* 14:e2021MS002954
106. Hersbach H, Bell B, Berrisford P, Hirahara S, Horányi A, et al. 2020. *Q. J. R. Meteorol. Soc.* 146:1999–2049
107. Bire S, Lütjens B, Azizzadenesheli K, Anandkumar A, Hill CN. 2023. **https://doi.org/10.22541/essoar.170110658.85641696/v1**
108. Subel A, Zanna L. 2024. arXiv:2402.04342 [physics.ao-ph]
109. Andersson TR, Hosking JS, Pérez-Ortiz M, Paige B, Elliott A, et al. 2021. *Nat. Commun.* 12:5124
110. Wang Y, Yuan X, Ren Y, Bushuk M, Shu Q, et al. 2023. *Geophys. Res. Lett.* 50:e2023GL104347
111. Zhu Y, Qin M, Dai P, Wu S, Fu Z, et al. 2023. *J. Geophys. Res. Atmos.* 128:e2023JD039521
112. Chattopadhyay Ashesh SYQ, Hassanzadeh P. 2023. arXiv:2304.07029 [physics.flu-dyn]
113. Selz T, Craig GC. 2023. *Geophys. Res. Lett.* 50:e2023GL105747
114. Kashinath K, Mustafa M, Wu J, Jiang C, Wang R, et al. 2021. *Philos. Trans. R. Soc. A* 379:20200093
115. Beucler T, Pritchard M, Rasp S, Ott J, Baldi P, Gentine P. 2021. *Phys. Rev. Lett.* 126:098302
116. Chattopadhyay A, Mustafa M, Hassanzadeh P, Bach E, Kashinath K. 2022. *Geosci. Model Dev.* 15:2221–37
117. Guan Y, Subel A, Chattopadhyay A, Hassanzadeh P. 2023. *Phys. D Nonlinear Phenom.* 443:133568
118. Psaros AF, Meng X, Zou Z, Guo L, Karniadakis GE. 2023. *J. Comput. Phys.* 477:111902
119. Abdar M, Pourpanah F, Hussain S, Rezazadegan D, Liu L, et al. 2021. *Inform. Fusion* 76:243–97
120. Sonnewald M, Lguensat R. 2021. *J. Adv. Model. Earth Syst.* 13:e2021MS002496
121. Yik W, Sonnewald M, Clare MCA, Lguensat R. 2023. arXiv:2310.13916 [physics.ao-ph]
122. Mansfield LA, Sheshadri A. 2024. *J. Adv. Model. Earth. Syst.* 16(7):e2024MS004292
123. Sun YQ, Pahlavan HA, Chattopadhyay A, Hassanzadeh P, Lubis SW, et al. 2024. *J. Adv. Model. Earth Syst.* 16:e2023MS004145
124. Dräger S, Sonnewald M. 2024. arXiv:2402.13979 [cs.LG]
125. Guillaumin AP, Zanna L. 2021. *J. Adv. Model. Earth Syst.* 13:e2021MS002534
126. Foster D, Gagne DJ, Whitt DB. 2021. *J. Adv. Model. Earth Syst.* 13:e2021MS002474
127. Barnes EA, Barnes RJ. 2021. *J. Adv. Model. Earth Syst.* 13:e2021MS002575
128. Haynes K, Lagerquist R, McGraw M, Musgrave K, Ebert-Uphoff I. 2023. *Artif. Intel. Earth Syst.* 2:220061
129. Rahaman N, Baratin A, Arpit D, Draxler F, Lin M, et al. 2019. In *Proceedings of the 36th International Conference on Machine Learning, PMLR*. 97:5301–10
130. Xu ZQJ, Zhang Y, Luo T, Xiao Y, Ma Z. 2019. arXiv:1901.06523 [cs.LG]
131. Rybchuk A, Hassanaly M, Hamilton N, Doubrawa P, Fulton MJ, Martínez-Tossas LA. 2023. *Phys. Fluids* 35:126604
132. Ng J, Wang Y, Lai CY. 2024. arXiv:2407.17213 [cs.LG]
133. Wang Y, Lai CY. 2024. *J. Comput. Phys.* 504(C):112865
134. Tancik M, Srinivasan P, Mildenhall B, Fridovich-Keil S, Raghavan N, et al. 2020. *Adv. Neural Inf. Proc. Syst.* 33:7537–47
135. Wang S, Wang H, Perdikaris P. 2021. *Comput. Methods Appl. Mech. Eng.* 384:113938
136. Miloshevich G, Cozian B, Abry P, Borgnat P, Bouchet F. 2023. *Phys. Rev. Fluids* 8:040501
137. Lopez-Gomez I, McGovern A, Agrawal S, Hickey J. 2023. *Artif. Intel. Earth Syst.* 2:e220035
138. Rudy SH, Sapsis TP. 2023. *Phys. D Nonlinear Phenom.* 443:133570
139. Ragone F, Wouters J, Bouchet F. 2018. *PNAS* 115:24–29
140. Finkel J, Webber RJ, Gerber EP, Abbot DS, Weare J. 2021. *Mon. Weather Rev.* 149:3647–69
141. Subel A, Guan Y, Chattopadhyay A, Hassanzadeh P. 2023. *PNAS Nexus* 2:pgad015
142. Beucler T, Gentine P, Yuval J, Gupta A, Peng L, et al. 2024. *Sci. Adv.* 10:eadj7250
143. Shen Z, Sridhar A, Tan Z, Jaruga A, Schneider T. 2022. *J. Adv. Model. Earth Syst.* 14:e2021MS002631

Review in Advance. Changes may still occur before final publication.

Downloaded from www.annualreviews.org. University of Chicago Libraries (ar-129425) IP: 128.135.43.97 On: Tue, 03 Dec 2024 18:25:25

144. Sun YQ, Hassanzadeh P, Alexander MJ, Kruse CG. 2023. *J. Adv. Model. Earth Syst.* 15:e2022MS003585
145. Satoh M, Stevens B, Judt F, Khairoutdinov M, Lin SJ, et al. 2019. *Curr. Climate Change Rep.* 5:172–84
146. Mamalakis A, Barnes EA, Ebert-Uphoff I. *Artif. Intel. Earth Syst.* 1:e220012
147. Camps-Valls G, Reichstein M, Zhu X, Tuia D. 2020. In *IGARSS 2020–2020 IEEE International Geoscience and Remote Sensing Symposium*, *Waikoloa*, *HI*, pp. 3979–82. Piscataway, NJ: IEEE
148. Mayer KJ, Barnes EA. 2021. *Geophys. Res. Lett.* 48:e2020GL092092
149. Bommer PL, Kretschmer M, Hedström A, Bareeva D, Höhne MMC. 2024. *Artif. Intel. Earth Syst.* 3:e230074
150. Flora M, Potvin C, Mcgovern A, Handler S. 2023. *Artif. Intel. Earth Syst.* 3:e230018
151. Irrgang C, Boers N, Sonnewald M, Barnes EA, Kadow C, et al. 2021. *Nat. Mach. Intel.* 3:667–74
152. Sonnewald M, Lguensat R, Jones DC, Dueben PD, Brajard J, Balaji V. 2021. *Environ. Res. Lett.* 16:073008
153. Toms BA, Barnes EA, Ebert-Uphoff I. 2020. *J. Adv. Model. Earth Syst.* 12:e2019MS002002
154. Labe ZM, Barnes EA. 2022. *Earth Space Sci.* 9:e2022EA002348
155. Farge M. 1992. *Annu. Rev. Fluid Mech.* 24:395–458
156. Mallat S. 2016. *Philos. Trans. R. Soc. A Math., Phys. Eng. Sci.* 374:20150203
157. Olshausen BA, Field DJ. 1996. *Nature* 381:607–9
158. Bassetti S, Hutchinson B, Tebaldi C, Kravitz B. 2023. *J. Adv. Model. Earth Syst.* 16(10):e2023MS004194
159. Finn TS, Durand C, Farchi A, Bocquet M, Brajard J. 2024. arXiv:2406.18417 [cs.LG]
160. Zhou A, Hawkins L, Gentine P. 2024. arXiv:2405.00018 [cs.DC]
161. Mukkavilli SK, Civitarese DS, Schmude J, Jakubik J, Jones A, et al. 2023. arXiv:2309.10808 [cs.LG]
162. Gupta A, Sheshadri A, Roy S, Gaur V, Maskey M, Ramachandran R. 2024. arXiv:2406.14775 [physics.ao-ph]
163. Balaji V. 2021. *Philos. Trans. R. Soc. A* 379:20200085

Review in Advance. Changes may still occur before final publication.